УДК 629.735.017.83

SYNTHESIS AND APPLICATION OF HIGH-QUALITY CARBON NANOFIBERS TO INCREASE THE PERFORMANCE OF AIRCRAFT PARTS

SHAHVERDI HAMID REZA[1], BOER HASSANY MERHDAD[1]
[1]Tarbiat Modares University, Tehran, Iran

Modern carbon nanofibers (CNF), obtained from polyacrylonitrile (PAN), do not have high tensile strength. It is because there is still no understanding how the electroforming method affects the quality of CNF.

This paper investigates a process to obtain high-strength nanofibers with a carbon content of up to 90% by the method of electroforming. The research made it possible to obtain CNFs with a diameter of 150–500 nm with unique properties due to our CNF continuous and combined forms, which distinguishes our CNFs from existing ones when applied to composite materials. Such nanofibers, obtained by selecting the optimum stabilization temperature and carbonization regime, have homogeneous cross sections, and as a result of improving their mechanical properties, the aircraft structure performance can be substantially improved.

Key words: nanofibers, polyacrylonitrile, electroforming, solvent, stabilization temperature, carbonization regime, wave band, electron microscope.

INTRODUCTION

Electrospinning is a process to form nanofibers (NV) as a result of electrostatic forces acting on an electrically charged jet of a polymer solution or melt. The scheme of the EF process is shown on Fig. 1 [8, 10, 14–16].

Electrical voltage of 1...100 kV (typically: 10–60 kV) is applied to a polymer solution (melt) fed through a capillary by means of a dispenser. High voltage induces electric charges of the same sign in the polymer solution. This, as a result of Coulomb electrostatic interaction, leads the polymer solution to stretch into a thin jet. In the process of electrostatic drawing of the polymer jet, the jet can undergo a series of successive splittings into thinner jets with a certain ratio of viscosity values, surface tension, and electric charge density (or electrostatic field strength) in the fiber. The resulting jets cure by evaporation of the solvent or as a result of cooling, turning into fibers, and, under the action of electrostatic forces, drift to a grounded substrate having the opposite sign of the electric potential. A variant is possible when the capillary is grounded, and high voltage is applied to the deposition substrate. The precipitation electrode (collector) must have good electrical conductivity, but the electrode can have a different shape: the rod, plane or cylinder, can be solid or as a grid, solid, or liquid, stationary, or mobile.

BASIC PROVISIONS

The material used to make our nanofibres: polyacrylonitrile with a molecular weight of 100,000 g/mol, containing 94,6% monoacrylonitrile and 5,4% monomethylacryl, in a solution of 15% by weight polymer (product of the Polyacryl Isfahan factory, Iran).

The properties of the solvent (product of “Merck”, Germany) to produce nanofibers are shown in Table 1.

Table 1

The product manufactured by "Merck" (Germany)

Name	Density, g/cm^3	Boiling Temperature, °C	Saturated vapor pressure at 1 atm.	Surface tension coeff, N/m	Relative dielectric permitivity
Dimethylformamide	0,945	153	0,0045	0,036	37

To determine the viscosity of our polymer solution, a rotary device "Brookfield" model DV2 (USA) is used with rotation speed of 20 rpm. The crystallinity index of our nanofiber polyacrylonitrile is determined by the formula [2, 7]

$$CF = A_{173_0} / A_{224_3},$$

where A_{173_0} – the area under the curve of one carbonyl group with wave number 1730 cm^{-1};

A_{224_3} – the area under the curve of one nytril group with wave number 2240 cm^{-1}.

As the degree of nanofiber crystallization increases, the nanofiber's crystallinity index is determined by the formula

$$CP = A_{224_3} / A_{173_0} + A_{224_3}.$$

The distance between nanofiber crystals is determined by the formula

$$\theta = \lambda / 2 \sin \theta,$$

where λ – radiation wavelength;

θ – angle of incidence, mm.

The nanofiber crystal size is determined by the formula

$$LC = 0/9\lambda / \beta \cos \theta,$$

where β – the area of the crystal at half its height.

PROCESS TO PRODUCE CARBON NANOFIBERS BY THE ELECTROSPINNING METHOD

At the Electrospinning unit (Fig. 1**)**, the voltage between the pump and the rotor collector is regulated within 12...25 kV. The distance between them should be 15...20 cm. The pump (volume 0,1 ml/h) sprays the solution on the rotor at speed of 40 Hz. The resulting nanofilament should be left at room temperature for 24 hours, so that dimethylformamide evaporates from the surface of the nanofibers.

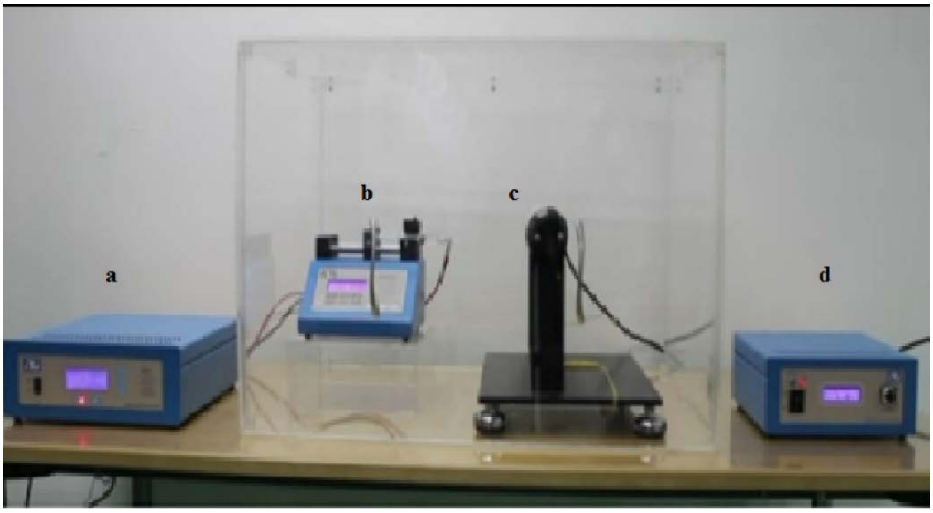

Fig. 1. Electrospinning plant:
a. High Voltage Source; b. Syringe Pump; c. Rotor Collector; d. Collector Controller

Voltage is regulated by a high voltage source. The collector and the pump are positioned at required distance. The syringe is filled with PAN and fixed on the pump. After that, the initial data is entered into the collector regulator. The liquid from the pump is sprayed onto the collector for 15 minutes.

HEAT TREATMENT OF PAN NANOFIBERS

Our PAN nanofibers were stabilized in a furnace (Thermolyne 47900) by heating to 300 °C with heating rate of 5 °C/min and holding for one hour at the maximum temperature. The optimal temperature and stabilization time are determined by differential scanning calorimetry. Stabilized nanofibers were deposited on alumina foil and placed in a high-temperature carbonization furnace.

Nitrogen is fed through the roof of the furnace and the nanofibers are heated for 1 hour under nitrogen (at peak temperatures of 800 °C, 1100 °C, 1400 °C, and 1700 °C) to determine how carbonization temperature influences the tensile strength and modulus of elasticity. The heating rate is 5°C/min. PAN and carbon nanofibers were tested for uniformity and presence of surface defects by means of a scanning electron microscope, while TEM was used to study the structure of nanofibers at different carbonization temperatures and to measure the average thickness of crystallite turbostratic carbon.

In this experiment, we investigated how the electroforming conditions influence the mechanical properties of PAN nanofibres to obtain a PAN with increased rigidity and strength.

INFLUENCE OF RELATIVE HUMIDITY ON THE MORPHOLOGY OF PAN NANOFIBERS

Relative humidity plays a critical role in obtaining a smooth surface of PAN nanofibres [8–9]. These nanofibers, formed at relative humidity of 60%, have a rough surface and porosity, while those made with 30% relative humidity had a smooth surface. Thus, the relative humidity is very important for our study to succeed.

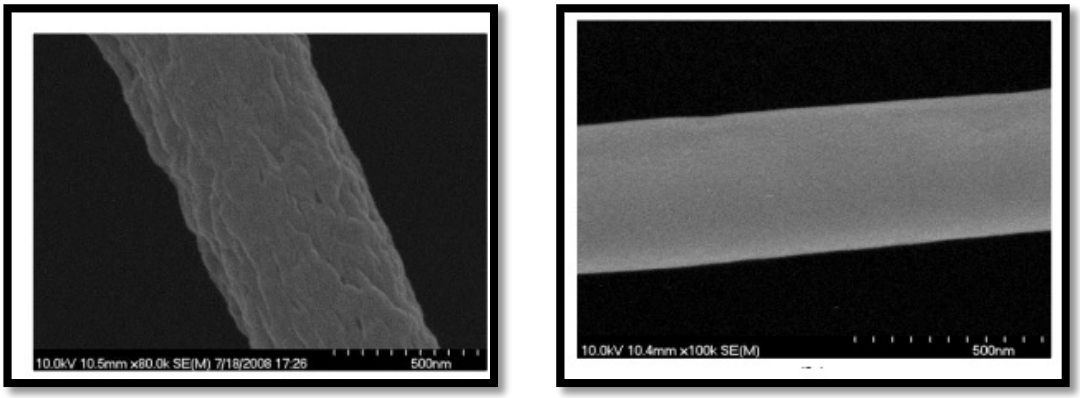

a. b.

Fig. 2. Nanofibers at humidity of 60% (a) and 30% (b). They have rough and smooth surfaces respectively

At high relative humidity, the solvent evaporates more slowly, which gives more time to produce nanofibers of smaller diameter and longer length.

RELATIONSHIP BETWEEN THE MECHANICAL PROPERTIES OF PAN NANOFIBERS AND THE ELECTROFORMING REGIME

In the course of our study, we determined optimal conditions for electroforming to improve molecular alignment and uniform cross-section of our nanofibers collected on a metal collector

[11–12, 16–17]. The effect of moisture was described in the previous section, but the effect of temperature and polymer concentration has not been studied. All work on electroforming was carried out at room temperature. Experimental conditions: the matrix of electrospinning voltage variation and the distance to the collector between 15...25 kV and 15...25 cm, respectively. At 15 kV and 25 cm, nanofibres were not obtained, probably because the surface charges on a drop of the polymer solution were insufficient to overcome the surface tension.

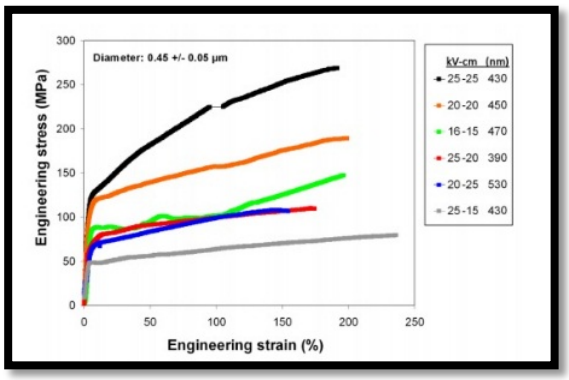

Fig. 3. Mechanical behavior of PAN nanofibers for different electrospinning conditions. The color code designations (in decreasing order) are voltage (kV), collector distance (cm) and nanofiber diameter (nm)

We isolated individual nanofibers by a heat probe made in the laboratory and tested by a nanoscale method of Naraghi (Fig. 3).

Fig. 3 shows stress-strain relationships for some of the electroforming processes. It can be seen that the mechanical strength of our nanofibers increases, depending on the electroforming data. The nanofilms, obtained at 25 kV and 25 cm from the collector, had the highest tensile strength and modulus of elasticity, although the fracture strain was ~ 200% relative to all the electroforming modes.

Stabilization is important to form a three-dimensional carbon grid that is thermally stable in subsequent carbonation and graphitization treatments. During stabilization and coking, the nanofibers were under stress to obtain high mechanical strength and high modulus of elasticity.

Stabilization was carried out at 270, 290, 300 °C with an increase in the thermal coefficient of 5 °C/min for one hour. The stabilization process is exothermic, so the amount of heat released depends on the time and degree of completeness of the reaction. As shown in Fig. 4, at 250 °C, and 275 °C, the exothermic reaction was not completed and the samples continued to generate heat for another 1 hour. However, the reaction was completed after 1 hour at 300 °C. The heat release was significantly higher than at 250 °C and 270 °C. The second stage was carried out at 300 °C, and during this stage no additional heat was released. This fact confirmed that the samples were stabilized during the first heating cycle. However, for the stabilization process, it is impossible to select high temperatures, so this will cause the fibers to combust.

For carbonization, stabilized nanofibers undergo heat treatment at 800–1700 °C until the carbon nanofibers are produced. The nanofilms are loaded into the furnace and partly covered to minimize the damaging effects of the convection processes that takes place in the furnace. We conducted FTIR spectroscopy on the PAN structure and found that the structure, along with stabilization and carbonization regimes, of our nanofibers changed in the right direction. The mechanical properties of each process (stabilization, carbonization, production of PAN nanofibres) are shown on Figure 5.

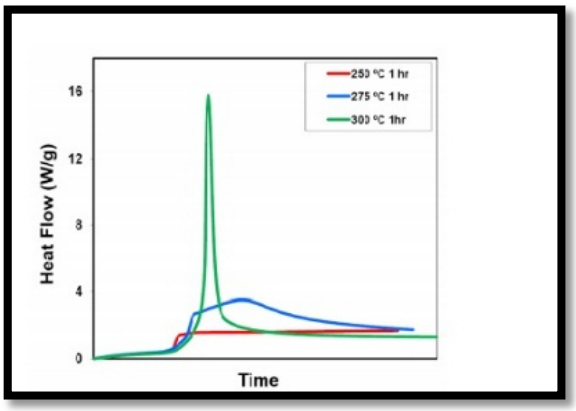

Fig. 4. DSC scans of PAN nanofibers stabilized at 250 °C, 275 °C, and 300 °C for 1 hr.

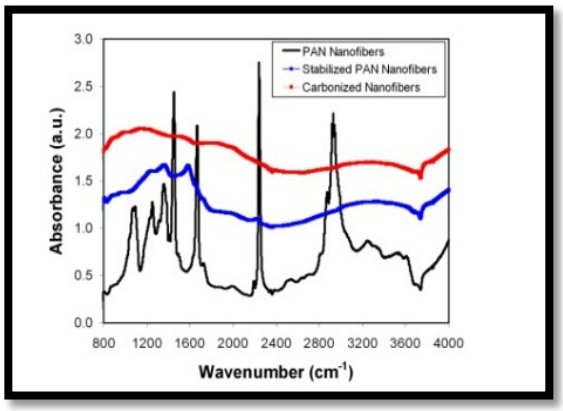

Fig. 5. FTIR spectra of PAN nanofibers shaping at 300 °C, stabilized nanofibers, and nanofibers carbonized at 800 °C

Figure 6 SEM depicts our carbon nanofibers that have a uniform structure, a smooth surface, and a uniform diameter along their entire length.

To study the thermal behavior of our polyacrylonitrile nanofibers, obtained by the EF method and the carbonization process, we use thermogravimetric analysis. When PAN nanowires are heated to 100–120 °C, a gentle slope occurs, along with a weight loss [3–5, 16–17]. This happens because the moisture inside the samples gets released and evaporated. Further, to stabilize the samples, we increase the temperature by 290 °C ± 20 °C. The carbonization process starts from 800 °C.

To study the shape and surface characteristics of our nanofibers, an electron microscope (SEM) was used. Fig. 6 shows that the diameter of each fiber reaches 500 nanometers. All nanofibers are homogeneous and lie in one direction; this is achieved by correctly setting the parameters of the EF installation and the optimal physical and chemical properties of the solution.

Figure 7, b shows that our nanofibers do not shrink in diameter, since they absorb sufficient amount of oxygen from the air. But the very structure of the macromolecule of polyacronitrile has changed, which becomes annular. The ring structures do not melt during the carbonization process and therefore retain their diameter.

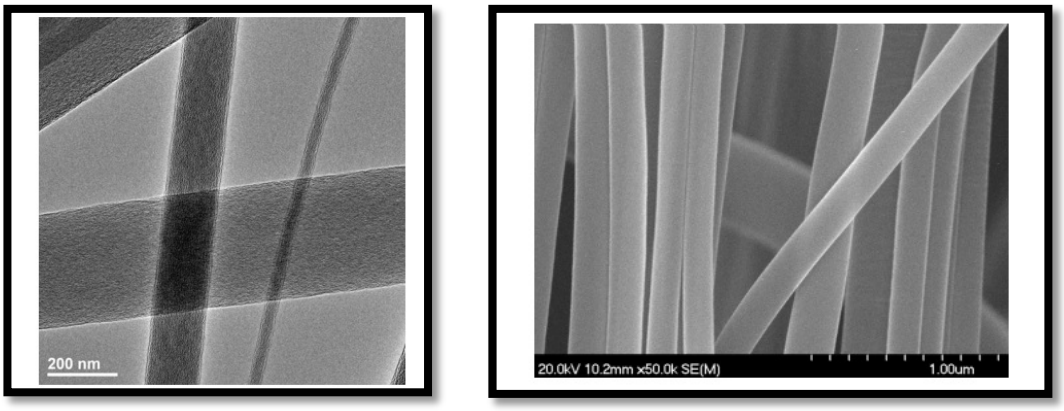

a. b.

Fig. 6. SEM image demonstrates alignment of continuous carbon nanofibers (a).
TEM image demonstrates the range of carbon nanofiber diameters
with homogeneous cross-sections without any evidence of skin-core structure (b)

At the stage of carbonization and raising the temperature to 1700 °C, the diameter of the fibers decreases because H2O and gases NCN, H2 escape, and the carbon content increases to 90%.

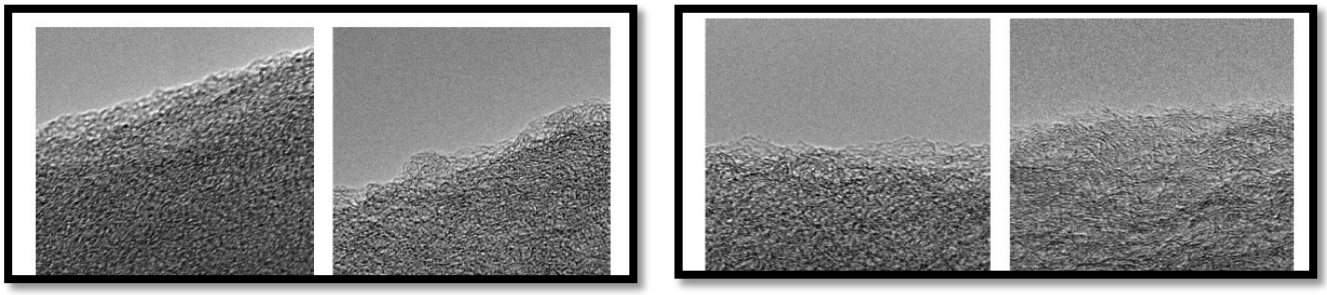

a. b. c. d.

Fig. 7. Polyacrylonitrile nanofibers obtained by electrospinning (a), b-stable nanofibers at 290 ±20 °C (b),
carbonation of nanofibers at 800 °C (c), stable carbon nanofibers at 1700 °C (d)

Vibrations of aliphatic CH groups were observed in the spectral regions 2870–2931, 1450–1460, 1350–1380, and 1220–1270. A strong band of absorption appeared in 2240 in conjunction with the group of triple CN nitrile. The band 1070 belongs to the group C and to the triple group CN.

Band 1732 refers to the bond length of excess vibrations of group C and the triple group CN. As a result, it is possible to detect if ester or acids are present. Two-band carbon materials have their own characteristics. Fig. 9 shows the spectrum of Raman scattering of carbon nanofibers.

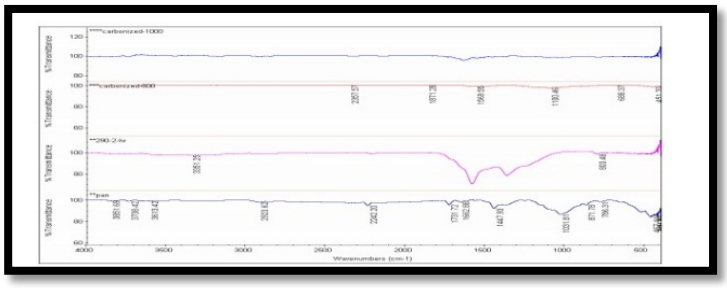

Fig. 8. Samples of spectra at various stages of our carbon nanofiber production process

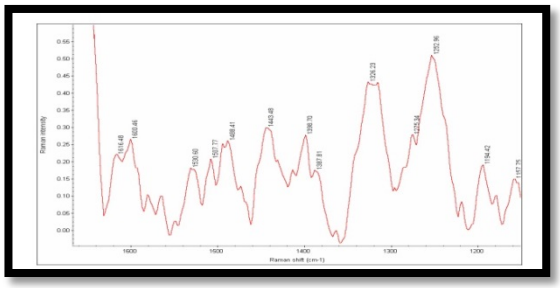

Fig. 9. Carbon nanofiber dispersion range

Thus, spectroscopy and its combinations are the most powerful tool to investigate microstructures, as can be seen from Table 2.

Table 2

The spectrum of the samples at various stages of the production process

Bonds	Wave number
OH bond oscillations indicating the water content Vibrations of the CH group with different aliphatic regimes CH and CH2	3500–3560
CH group vibrations with different aliphatic regimes CH and CH2	2900
The relative triple bond CN	2242
Carbon monoxide and nitrogen carbon group, double bond	1731
Group C-H and bending CH2 bond	452–1447
Relative C-C bond and double N bond	1071

TENSILE STRENGTH AND MODULUS OF ELASTICITY OF CARBON NANOFIBERS

The ultimate strength of our nanofiber at four temperatures is shown in Fig. 10, a. The plot shows how the carbonization temperature is related to the ultimate strength; this information allows us to tune the carbonization process for maximum performance [3–4, 8]. The maximum strength is achieved at temperatures up to 1400 °C. After this value (1400–1700 °C), the strength decreases. Fig. 10, b is the average number of nanofibers vs. carbonization temperature plot. The required diameter is obtained at low carbonation temperatures. Similarly, the modulus of elasticity depends on the diameter of the nanofiber, as shown on Fig. 11, a, and the modulus increases as the temperature increases, as shown on Fig. 11, b. The elastic modulus increases as the crystallite thickness and length increases.

As noted, the diameter increases as the sample is stretched and as the sample's tensile strength slightly decreases at low carbonation temperatures of 800 °C and 1100 °C. The strength limit increases by almost 150% at 800°C for carbonized nanofibers when the diameter was reduced from 500 nm to 200 nm.

The images of our samples, obtained at different carbonization temperatures, are shown on Fig. 11 (b). No porosity or other discernible defects were detected, except for a slight surface roughness. A study of the mechanical properties of PAN nanofibers on Naraghi shows that nanofibers with a larger diameter had less strength and reduced molecular alignment.

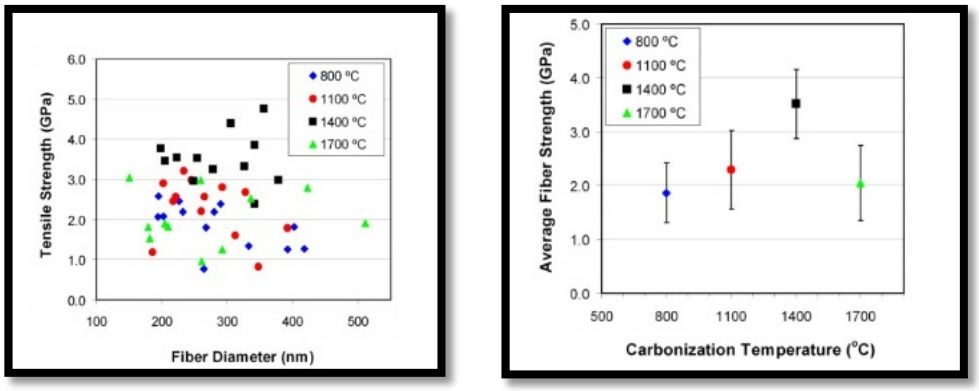

a. b.

Fig. 10. The dependence of the tensile strength and the diameter of the Nanofibers during carbonation (at different temperature values) (a). The dependence of the average number of Nanofibers on carbonization temperature (b)

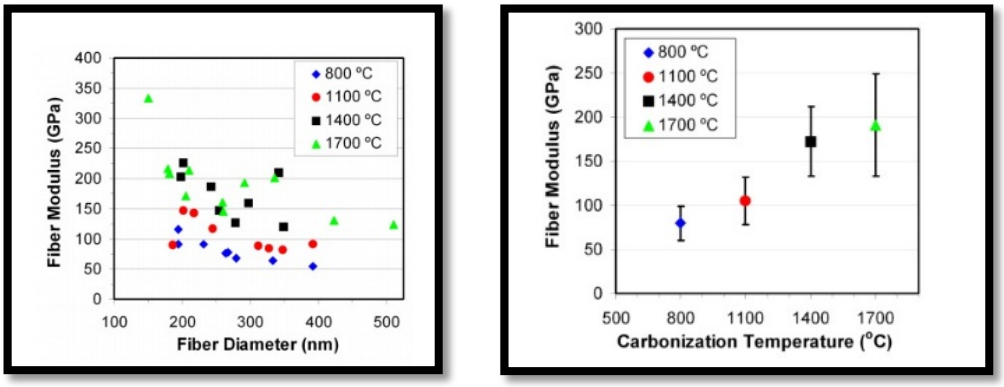

a. b.

Fig. 11. The dependence of the elasticity modulus on the diameter of Nanofibers (a), dependence of the average level of the elasticity modulus on the carbonization temperature (b)

The nanofilms, carbonized at 1400 °C, obtain fiber strength of 3.60 GPa. The normative strength in this case increases by a factor of 6, compared to the average strength. Nevertheless, the strength of nanofibers carbonized at 1700 °C decreases sharply at break. In this paper, we already demonstrated that the optimal molecular alignment prior to the stabilization process was important, whereas the non-uniform structure of the core was absent. This process was identified as a limiting factor for achieving high mechanical strength. The mechanical strength decreases as the crystalline structure of nanofibers develops. As the carbonization temperature increases, turbo nanocarbon forms up. This caused the sample to rupture since there is a discrepancy between the stresses of turbostratic carbon and the stress of amorphous carbon, that surrounds the turbostratic one.

A large number of images of carbon nanofibers were obtained to measure the average crystallite thickness. This allowed us to estimate how the crystallite thickness changes, Lc, and the length of La. Lc and La increase as carbonization temperature increases. As indicated in Table 3, the average crystallite thickness increased by 3.3±0.9 layers (on average) at 800 °C, and by 7.9±1.9 layers (on average) at 1700 °C.

Table 3

Features of fiber strength modulus depending on carbonization temperature

Carbonization temperature, °C	Carbone content, %	Strength index, GPa	Elasticity modulus, GPa	Average crystallite value
800	81,2	2,20	80±19	3,3±0,9
1100	92,7	2,90	105±27	3,9±0,9

Table continuation

1400	N/A	3,60	172±40	6,6±1,4
1700	N/A	1,95	191±58	7,9±1,9

CONCLUSIONS

To study the thermal behavior and carbonization of PAN nanofibers, obtained by the EF method, the thermogravimetry analysis was used. When PAN nanowires are heated to 100–120 °C, a gentle slope with a weight loss occurs. This is due to the moisture gets released and evaporated. Further, to stabilize the process, the temperature was raised to 290±20 °C. The carbonization process starts at 800 °C.

Our CNF, described in this paper, are unique in comparison with the existing carbon nanofibers and nanotubes because of these CNF have continuous and combined forms, which are advantageous when used in composite materials. The ultimate strength of carbon nanofibers reaches a maximum of 3.6 GPa at 1400 °C, the modulus of elasticity increases to 1700 °C and is equal to 172 ± 40 GPa, which is 600% and almost 300%, respectively, relative to the previously reported data. This improvement is a result of our effort to stabilize temperature and carbonization. So, our carbon nanofibers have uniform cross-sections and as a result - improved mechanical properties, which allow to increase the efficiency of aircraft structures.

REFERENCES

1. Chan C.K., Patel R.N., O'Connell M.J., Korgel B.A., Y. Cui. Solution-grown silicon nanowires for lithium-ion battery anodes. ACS Nano, vol. 4, no. 3, pp. 1443–1450, 2010.

2. Yoo J.-K., Kim J., Jung Y.S., Kang K. Scalable fabrication of silicon nanotubes and their application to energy storage. Advanced Materials, vol. 24, no. 40, pp. 5452–5456, 2012.

3. Lee B.H., Song M.Y., Jang S.-Y., Jo S.M., Kwak S.-Y., Kim D.Y. Charge transport characteristics of high efficiency dye-sensitized solar cells based on electrospun TiO_2 nanorod photoelectrodes. The Journal of Physical Chemistry C, vol. 113, no. 51, pp. 21453–21457, 2009.

4. Liu Y., Goebl J., Yin Y. Templated synthesis of nanostructured materials. Chemical Society Reviews, vol. 42, no. 7, pp. 2610–2653, 2013.

5. Chi M., Zhao Y., Fan Q., Han W. The synthesis of PrB_6 nanowires and nanotubes by the self-catalyzed method. Ceramics International, vol. 40, no. 6, pp. 8921–8924, 2014.

6. Kovtyukhova N.I., Martin B.R., Mbindyo J.K.N., Mallouk T.E., Cabassi M., Mayer T.S. Layer-by-layer self-assembly strategy for template synthesis of nanoscale devices. Materials Science and Engineering: C, vol. 19, no. 1–2, pp. 255–262, 2002.

7. Zhu H., Gao X., Lan Y., Song D., Xi Y., Zhao J. Hydrogen titanate nanofibers covered with anatase nanocrystals: a delicate structure achieved by the wet chemistry reaction of the titanate nanofibers. Journal of the American Chemical Society, vol. 126, no. 27, pp. 8380–8381, 2004.

8. Jayaraman S., Aravindan V., Suresh Kumar P., Ling W.C., Ramakrishna S., Madhavi S. Synthesis of porous $LiMn_2O_4$, PAN hollow nanofibers by electrospinning with extraordinary lithium storage properties. Chemical Communications, vol. 49, no. 59, pp. 6677–6679, 2013.

9. Ramakrishna S., Jose R., Archana P.S. et al. Science and engineering of electrospun nanofibers for advances in clean energy, water filtration, and regenerative medicine Journal of Materials Science, vol. 45, no. 23, pp. 6283–6312, 2010.

10. Zhang X., Aravindan V., Kumar P.S. et al. Synthesis of TiO_2 hollow nanofibers by coaxial electrospinning and its superior lithium storage capability in full-cell assembly with olivine phosphate. Nanoscale, vol. 5, no. 13, pp. 5973–5980, 2013.

11. Engstrom D.S., Porter B., Pacios M., Bhaskaran H. Additive nanomanufacturing - a review Journal of Materials Research, vol. 29, no. 17, pp. 1792–1816, 2014.

12. Park J.U., Hardy M., Kang S.J. et al. High-resolution electrohydrodynamic jet printing. Nature Materials, vol. 6, no. 10, pp. 782–789, 2007.

13. Galliker P., Schneider J., Eghlidi H., Kress S., Sandoghdar V., Poulikakos D. Direct printing of nanostructures by electrostatic autofocussing of ink nanodroplets. Nature Communications, vol. 3, article 890, 2012.

14. Yao S., Wang X., Liu X., Wang R., Deng C., Cui F. Effects of ambient relative humidity and solvent properties on the electrospinning of pure hyaluronic acid nanofibers. Journal of Nanoscience and Nanotechnology, vol. 13, no. 7, pp. 4752–4758, 2013.

15. Vrieze S., T. van Camp, Nelvig A., Hagström B., Westbroek P., K. de Clerck. The effect of temperature and humidity on electrospinning. Journal of Materials Science, vol. 44, no. 5, pp. 1357–1362, 2009.

16. Casasola R., Thomas N.L., Trybala A., Georgiadou S. Electrospun poly lactic acid (PLA) fibres: effect of different solvent systems on fibre morphology and diameter. Polymer, vol. 55, no. 18, pp. 4728–4737, 2014.

17. Yang Q., Li Z., Hong Y. et al. Influence of solvents on the formation of ultrathin uniform poly (vinyl pyrrolidone) nanofibers with electrospinning. Journal of Polymer Science Part B: Polymer Physics, vol. 42, no. 20, pp. 3721–3726, 2004.

INFORMATION ABOUT THE AUTHORS

Shahverdi Hamid Reza, Doctor of Material Science, Tarbiat Modares University, CEO of Mobin Company, Shahverd@modares.ac.ir.

Boer Hassany Merhdad, Engineer of the manufacturing airplanes and helicopters, M.Boyerhassani@gmail.com.

ПОЛУЧЕНИЕ И ПРИМЕНЕНИЕ ВЫСОКОКАЧЕСТВЕНОГО УГЛЕРОДНОГО НАНОВОЛОКНА ДЛЯ ПОВЫШЕНИЯ РАБОТОСПОСОБНОСТИ ДЕТАЛЕЙ ВОЗДУШНЫХ СУДОВ

Шахверди Хамид Реза[1], Боер Хассани Мехрдад[1]
[1]Университет Тарбиат Модарес, г. Тегеран, Иран

Полученные из полиакрилонитрила (ПАН) современные углеродные нановолокна (УНВ) не обладают пока высокой прочностью при растяжении. Это связано с отсутствием в настоящее время понимания того, как влияет метод электроформования на качество УНВ.

В статье рассмотрен процесс получения высокопрочного нановолокна с содержанием углерода до 90 % методом электроформования. Проведенные исследования позволили получить УНВ диаметром 150–500 нм с уникальными свойствами, обусловленными их непрерывными и совмещенными формами, что выгодно отличает их от существующих при применении в композиционных материалах. Такие нановолокна, полученные путем выбора оптимальной температуры стабилизации и режима карбонизации, имеют однородные поперечные сечения, и в результате улучшения их механических свойств может быть существенно повышена работоспособность авиационных конструкций.

Ключевые слова: нановолокно, полиакрилонитрил, электроформование, растворитель, температура стабилизации, режим карбонизации, диапазон волн, электронный микроскоп.

СПИСОК ЛИТЕРАТУРЫ

1. Chan C.K., Patel R.N., O'Connell M.J., Korgel B.A., Y. Cui. Solution-grown silicon nanowires for lithium-ion battery anodes. ACS Nano, vol. 4, no. 3, pp. 1443–1450, 2010.

2. Yoo J.-K., Kim J., Jung Y.S., Kang K. Scalable fabrication of silicon nanotubes and their application to energy storage. Advanced Materials, vol. 24, no. 40, pp. 5452–5456, 2012.

3. Lee B.H., Song M.Y., Jang S.-Y., Jo S.M., Kwak S.-Y., Kim D.Y. Charge transport characteristics of high efficiency dye-sensitized solar cells based on electrospun TiO_2 nanorod photoelectrodes. The Journal of Physical Chemistry C, vol. 113, no. 51, pp. 21453–21457, 2009.

4. Liu Y., Goebl J., Yin Y. Templated synthesis of nanostructured materials. Chemical Society Reviews, vol. 42, no. 7, pp. 2610–2653, 2013.

5. Chi M., Zhao Y., Fan Q., Han W. The synthesis of PrB_6 nanowires and nanotubes by the self-catalyzed method. Ceramics International, vol. 40, no. 6, pp. 8921–8924, 2014.

6. Kovtyukhova N.I., Martin B.R., Mbindyo J.K.N., Mallouk T.E., Cabassi M., Mayer T. S. Layer-by-layer self-assembly strategy for template synthesis of nanoscale devices. Materials Science and Engineering: C, vol. 19, no. 1–2, pp. 255–262, 2002.

7. Zhu H., Gao X., Lan Y., Song D., Xi Y., Zhao J. Hydrogen titanate nanofibers covered with anatase nanocrystals: a delicate structure achieved by the wet chemistry reaction of the titanate nanofibers. Journal of the American Chemical Society, vol. 126, no. 27, pp. 8380–8381, 2004.

8. Jayaraman S., Aravindan V., Suresh Kumar P., Ling W.C., Ramakrishna S., Madhavi S. Synthesis of porous $LiMn_2O_4$ hollow nanofibers by electrospinning with extraordinary lithium storage properties. Chemical Communications, vol. 49, no. 59, pp. 6677–6679. 2013.

9. Ramakrishna S., Jose R., Archana P.S. et al. Science and engineering of electrospun nanofibers for advances in clean energy, water filtration, and regenerative medicine Journal of Materials Science, vol. 45, no. 23, pp. 6283–6312, 2010.

10. Zhang X., Aravindan V., Kumar P.S. et al. Synthesis of TiO_2 hollow nanofibers by coaxial electrospinning and its superior lithium storage capability in full-cell assembly with olivine phosphate. Nanoscale, vol. 5, no. 13, pp. 5973–5980, 2013.

11. Engstrom D.S., Porter B., Pacios M., Bhaskaran H. Additive nanomanufacturing – a review Journal of Materials Research, vol. 29, no. 17, pp. 1792–1816, 2014.

12. Park J.U., Hardy M., Kang S.J. et al. High-resolution electrohydrodynamic jet printing. Nature Materials, vol. 6, no. 10, pp. 782–789, 2007.

13. Galliker P., Schneider J., Eghlidi H., Kress S., Sandoghdar V., Poulikakos D. Direct printing of nanostructures by electrostatic autofocussing of ink nanodroplets. Nature Communications, vol. 3, article 890, 2012.

14. Yao S., Wang X., Liu X., Wang R., Deng C., Cui F. Effects of ambient relative humidity and solvent properties on the electrospinning of pure hyaluronic acid nanofibers. Journal of Nanoscience and Nanotechnology, vol. 13, no. 7, pp. 4752–4758, 2013.

15. Vrieze S., T. van Camp, Nelvig A., Hagström B., Westbroek P., K. de Clerck. The effect of temperature and humidity on electrospinning. Journal of Materials Science, vol. 44, no. 5, pp. 1357–1362, 2009.

16. Casasola R., Thomas N.L., Trybala A., Georgiadou S. Electrospun poly lactic acid (PLA) fibres: effect of different solvent systems on fibre morphology and diameter. Polymer, vol. 55, no. 18, pp. 4728–4737, 2014.

17. Yang Q., Li Z., Hong Y. et al. Influence of solvents on the formation of ultrathin uniform poly (vinyl pyrrolidone) nanofibers with electrospinning. Journal of Polymer Science Part B: Polymer Physics, vol. 42, no. 20, pp. 3721–3726, 2004.

СВЕДЕНИЯ ОБ АВТОРАХ

Шахверди Хамид Реза, доктор технических наук, университет Тарбиат Модарес, генеральный директор компании «Мобин», Shahverd@modares.ac.ir.

Боер Хассани Мерхдад, инженер по производству самолетов и вертолетов, M.Boyerhassani@gmail.com.

Поступила в редакцию	19.01.2017	Received	19.01.2017
Принята в печать	27.04.2017	Accepted for publication	27.04.2017